Quantum Electronics **46** (5) 453–463 (2016)

LASER SPECTROSCOPY DOI: 10.1070/QEL15989

New polarisation effects in saturated absorption spectroscopy in the field of counterpropagating light waves*

D.V. Brazhnikov, A.S. Novokreshchenov, S.M. Ignatovich, A.V. Taichenachev, V.I. Yudin

Abstract. **The effect of a double structure of saturated absorption resonance in the field of counterpropagating light waves interacting with atomic gas is considered, which was first studied experimentally and theoretically by Vasil'ev et al. [V.V. Vasil'ev et al., *J. Exp. Theor. Phys*., 112, 770 (2011)]. The effect manifests itself as a new nonlinear resonance formed as a peak in the absorption spectrum of the probe wave. The resonance is observed inside a 'conventional' dip in the spectrum of saturated absorption. Previously, this effect was theoretically described only in the frameworks of the two-level atomic model, i.e., without making allowance for degeneracy of atomic energy levels with respect to the projection of the total angular momentum and for the vector nature of light. We extend the theory of the effect to the case of real atomic systems with degenerate energy levels and arbitrary polarisations of light waves. In particular, on an example of the simple transition $F_g = 1 \rightarrow F_e = 0$ we show that polarisation parameters of light waves may significantly affect the contrast of the new effect and the possibility of observing it at all. Conclusions of the work are confirmed both analytically and bnumerically.**

Keywords: *saturated absorption resonance, elliptical polarisation, quantum metrology, high-resolution spectroscopy, density matrix.*

1. Introduction

With invention of lasers, nonlinear spectroscopy of gases was given a second birth (see, for example, monographs [1–3]). This field of physics is intensively developing due to its importance for fundamental science and for numerous practical applications. One of the main fundamental phenomena in the field of nonlinear laser spectroscopy of gases is saturated absorption resonance (SAR). Presently, there is a great number of works devoted to versatile investigations of this resonance in various configurations of electromagnetic fields (see, for example, first basic papers [4–6] and monographs [1, 2]).

Mostly, SAR is studied and practically employed in the configuration of two counterpropagating light waves of the same frequency interacting with a common electro-dipole atomic (molecular) transition. As a rule, SAR is observed as a single structure in the absorption spectrum of one of the waves (probe), that is, either a dip or a peak is observed at the centre of a wide-band Doppler profile, depending on the polarisation of the counterpropagating waves and on the structure of atomic energy levels [7, 8].

Despite the fact that the main experimental and theoretical investigations of SAR were performed in the 1960s and 1970s, recently principally new features of this resonance have been discovered. In a theoretical work [9], a new 'source' of the shift of nonlinear resonance was found, which was related to polarisation parameters of the light waves. Another new effect in saturation spectroscopy was a contrast double structure of SAR observed in 2010 at the P.N. Lebedev Physics Institute of RAS [10]. The formation of this structure comprised of a 'conventional' dip in the spectrum of saturated absorption and a narrower central peak could not be explained by effects known earlier (the recoil effect [11], the influence of higher spatial harmonics of atomic polarisation [12], the presence of a residual external magnetic field [13, 14], the effects arising in strong fields [15, 16], etc). An example of the double SAR structure is shown in Fig. 1.

New data on the saturation effect obtained in [9, 10] are important, for example, from the viewpoint of quantum metrology for creating frequency standards based on SAR. The most widely known optical frequency standards (including transportable ones) are He–Ne and Nd:YAG lasers stabilised by SAR on vibrational–rotational transitions of methane and iodine molecules (see, for example, [17–20]). There are also publications where the frequency of laser radiation is stabilised by SAR, for example, in vapours of alkali metals (rubidium [21] and caesium [22, 23]), including stabilisation of frequency combs [24]. In addition, in many spectroscopic experiments, SAR plays an auxiliary role for matching the frequency of laser radiation with a desired spectral line in gases. Also, the method of saturated spectroscopy gives a chance to observe and study quantum and relativistic effects (the recoil effect [11, 25, 26] and pressure of light [27], the quadratic Doppler effect [28], the quantum bistability effect in a cavity [29], and other) as well as the effects of atom scattering in gas [30].

* Reported at The Fifth Russia–China Workshop on Laser Physics and Photonics (RCWLP&P, Novosibirsk, 26–30 August 2015).

D.V. Brazhnikov, A.V. Taichenachev Institute of Laser Physics, Siberian Branch, Russian Academy of Sciences, prosp. Akad. Lavrent'eva 13/3, 630090 Novosibirsk, Russia; Novosibirsk National Research State University, ul. Pirogova 2, 630090 Novosibirsk, Russia; e-mail: brazhnikov@laser.nsc.ru;
A.S. Novokreshchenov, S.M. Ignatovich Institute of Laser Physics, Siberian Branch, Russian Academy of Sciences, prosp. Akad. Lavrent'eva 13/3, 630090 Novosibirsk, Russia;
V.I. Yudin Institute of Laser Physics, Siberian Branch, Russian Academy of Sciences, prosp. Akad. Lavrent'eva 13/3, 630090 Novosibirsk, Russia; Novosibirsk State Technical University, prosp. Karla Marksa 20, 630073 Novosibirsk, Russia; Novosibirsk National Research State University, ul. Pirogova 2, 630090 Novosibirsk, Russia

Received 7 December 2015
Kvantovaya Elektronika **46** (5) 453–463 (2016)
Translated by N.A. Raspopov

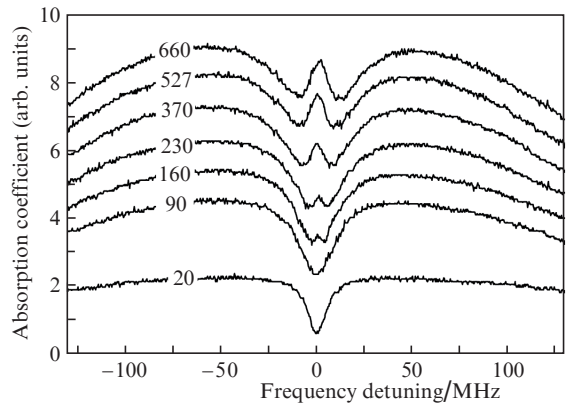

Figure 1. Coefficient of the probe wave absorption vs. detuning of the laser frequency from the transition frequency [10]. The power of the counterpropagating wave is 90 μW, the power of the probe wave is shown near the curves (in μW). The diameter of a light beam in a cell is 10 mm.

All the applications mentioned above confirm the importance of the new knowledge about the saturation effect for atomic and molecular transitions and resonances related to the latter. In particular, the new contrast nonlinear resonance discovered in [10] in the form of a peak at the centre of an absorption line (Fig. 1) can be used instead of a conventional dip in the spectrum of saturated absorption for stabilising the frequency of laser radiation in cases of open atomic transitions, because the new resonance can be several times narrower than SAR.

The present work is devoted to development of a theory of the new nonlinear resonance that has been observed for the first time in [10]. Here we pay a particular attention to the polarisation aspect of the interaction between atoms and the field of laser radiation. The fact is that for qualitative understanding of the physics of the new phenomenon, a simplified two-level model of atom was used in [10], which made no allowance for degeneracy of atomic levels with respect to projections of the total angular momentum and for the vector nature of light. This approach was useful in establishing the following conditions needed for observing the contrast double structure of SAR:

1) the atomic transition should be open;

2) the more intensive wave should be monitored (from the two counterpropagating waves).

Whereas the first condition is often fulfilled in practice (especially for molecules), the second condition conventionally is not. In other words, in most works mainly two cases of counterpropagating wave intensities are studied: the regime of a standing wave, where the two waves have equal intensities, and the so-called pump-probe regime when the intensity of the observed wave ('probe') is noticeably lower than that of the counterpropagating wave ('pumping'). In our opinion, it is the failure of the second condition that has prevented investigation of the new effect for a long time.

Despite the fact that the two-level model of the atom used in [10] was useful in establishing the main laws of the new effect, there are still unsolved problems. In particular, this model may be rather rough because in experiments on SAR observation, real atomic transitions always comprise levels degenerated with respect to the projection of the total angular momentum, and the beams of laser radiation have certain polarisations. Hence, the model suggested in [10] can hardly describe the effect of the SAR double structure. Moreover, neglected influence of light wave polarisations may substantially affect the contrast of the double structure in real experiments. Indeed, it is known that the parameters of light field polarisation strongly affect nonlinear resonances in atomic gases (see, for example, [7–9, 31–33]). Thus, for better understanding of the physics of the new nonlinear effect (the double structure of SAR) it is necessary to extend the theory [10] as applied to the case of real atomic transitions and accurately take into account the polarisations of the counterpropagating light waves.

The theoretical analysis of this problem performed in the present work is based on the standard formalism of the single-atom density matrix (the light field is assumed classical). As an example, we consider a comparatively simple atomic transition with a degenerated ground state: $F_g = 1 \rightarrow F_e = 0$, where F_g and F_e are the angular momenta of the ground and excited states, respectively. For the simple configurations of laser field polarisations comprised of linearly or circularly polarised counterpropagating waves, analytical results have been obtained. For arbitrary elliptical polarisations numerical calculations were performed. In particular, a strong influence of the polarisation parameters on the contrast of the double SAR structure and on the possibility of observing the effect has been revealed. It was demonstrated that the first condition concerning the open transition established in [10] and mentioned above is not, strictly speaking, the necessary condition for observing the contrast SAR double structure.

Note that the polarisation effects on an example of the transition $F_g = 1 \rightarrow F_e = 0$ were repeatedly studied earlier. However, either the standing wave or the pumping-probe regimes have been most commonly considered (see, for example, [7]). Absorption of a light wave in this transition has been investigated in [34] for arbitrary ratios of the intensities of counterpropagating waves. Nevertheless, the problem has only been solved for orthogonal circular polarisations (the $\sigma^+\sigma^-$ configuration) and only in the frameworks of homogeneous broadening of atomic levels, which does not corresponds to atomic gas at room temperature; in addition, the case of the exact resonance (that is, the central point on a resonance curve) was considered, hence, the effect of double SAR structure has been lost. In the present work we consider various polarisation configurations and make allowance for the inhomogeneous broadening, which is principal for revealing the effect of the double SAR structure.

2. Problem statement

Consider the configuration of a laser field comprised of plane monochromatic waves counterpropagating along the quantization axis z in an atomic gas:

$$\boldsymbol{E}(z,t) = E_1\boldsymbol{e}_1\exp[-\mathrm{i}(\omega t - kz)] + E_2\boldsymbol{e}_2\exp[-\mathrm{i}(\omega t + kz)] + \text{c.c.} \quad (1)$$

Here E_j is the amplitude of the jth wave ($j = 1,2$), which is assumed real; and $\boldsymbol{e}_1$ and $\boldsymbol{e}_2$ are the complex unit polarisation vectors. Geometry of the laser field is shown in Fig. 2.

Interaction of atoms with a light field will be described by using the formalism of the density matrix $\hat{\rho}$ with the Lindblad-type equation [2, 35]:

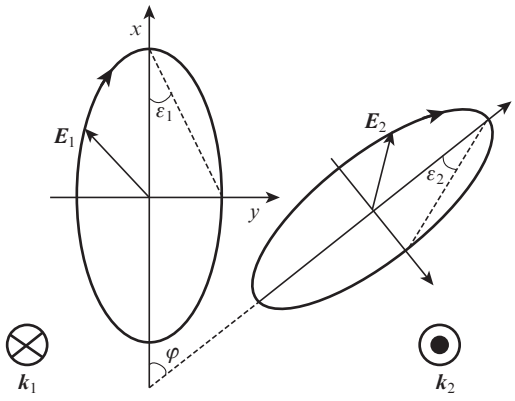

Figure 2. Mutual orientation of the polarisation ellipses for counterpropagating waves: $\boldsymbol{k}_1 = -\boldsymbol{k}_2 = \boldsymbol{k}$ are the wave vectors; ε_j are the parameters of ellipticity; and φ is the angle between the axes of the ellipses of the wave polarisation.

$$\left(\frac{\partial}{\partial t} + \boldsymbol{v}\nabla\right)\hat{\rho} = -\frac{\mathrm{i}}{\hbar}[\hat{H},\hat{\rho}] + \hat{\Gamma}\{\hat{\rho}\}, \tag{2}$$

where v is the vector of atom velocity; $\hat{H}$ is the Hamiltonian; and $\hat{\Gamma}$ is the operator, which describes relaxation processes in the atomic system. The Hamiltonian consists of two summands: $\hat{H} = \hat{H}_0 + \hat{V}_E$, here $\hat{H}_0$ is the Hamiltonian of the free atom and $\hat{V}_E$ is the operator of interaction of the atom with an external field in the electro-dipole approximation.

In the case of the two-level spectroscopic model of an atom, which was used in [10], the density matrix dimension was 2×2. In the case of a real atomic transition with angular momenta F_g and F_e the situation is much more complicated because the dimension of $\hat{\rho}$ can be substantially greater, and in the general form it is $2(F_g + F_e + 1) \times 2(F_g + F_e + 1)$. Then the density matrix can be conveniently divided to the matrix blocks:

$$\hat{\rho} = \begin{pmatrix} \hat{\rho}^{g} & \hat{\rho}^{ge} \\ \hat{\rho}^{eg} & \hat{\rho}^{e} \end{pmatrix}. \tag{3}$$

Diagonal elements of the matrices $\hat{\rho}^g$ and $\hat{\rho}^e$ describe the populations of magnetic ('Zeeman') sublevels of the ground and excited states, respectively, whereas off-diagonal elements refer to the mutual coherence of these states ('Zeeman' coherences). The blocks $\hat{\rho}^{ge}$ and $\hat{\rho}^{eg}$ are called the optical coherences (they oscillate in time at an optical frequency ω). In the present work we consider a stationary regime and use the approximation of the lowest spatial harmonics for atomic polarisation, which for the optical coherences means the expansion

$$\hat{\rho}^{eg}(z,t) = \hat{\tilde{\rho}}_1^{eg}\exp[-\mathrm{i}(\omega t - kz)] + \hat{\tilde{\rho}}_2^{eg}\exp[-\mathrm{i}(\omega t + kz)] + \text{H.c.} \tag{4}$$

where the matrices $\hat{\rho}^e$ and $\hat{\rho}^g$ are assumed independent of time and coordinates. For the scheme of counterpropagating monochromatic waves and in the regime of small saturation of the atomic transition this approximation is, as a rule, quite reasonable.

In the basis of a rotating wave, the operators $\hat{H}_0$ and $\hat{V}_E$ can be represented in the form

$$\hat{H}_0 = -\hbar\delta\hat{P}^e, \tag{5}$$

$$\hat{V}_E = -\hat{\boldsymbol{d}}\boldsymbol{E} = -\hbar R_1\hat{V}_1\exp(\mathrm{i}kz) - \hbar R_2\hat{V}_2\exp(-\mathrm{i}kz) + \text{H.c.}, \tag{6}$$

where $\delta = \omega - \omega_0$ is the frequency detuning of laser generation from the atomic transition; $\hat{P}^e$ is the projection operator to the excited atomic state; $\hat{\boldsymbol{d}}$ is the operator of the atomic dipole momentum; $R_j = dE_j/\hbar$ is the Rabi frequency corresponding to the jth wave; d is the reduced matrix element of the operator of the atomic dipole momentum; and $\hat{V}_j$ are the dimensionless operators of interaction of the atom with a laser field, related to the Clebsch–Gordan coefficients [36]. For shortness, we will not thoroughly discuss here the mathematical approach used. One can find details of the formalism in [9].

In the present work we assume that there are two main relaxation processes in the atom: the spontaneous relaxation of the excited level F_e and the 'flight' relaxation related to the departure of atoms from the zone of interaction with the resonance light field. These processes will be described in the frameworks of the model of relaxation constants (γ and Γ, respectively).

Consider an absorption spectrum of one of the counterpropagating waves, which we will conditionally call the probe wave (not implying that its intensity is less than that of the counterpropagating wave). From the reduced Maxwell equation it follows that the intensity of this wave in medium varies according to the law

$$\frac{\mathrm{d}I_2}{\mathrm{d}z} = -\alpha(I_1, I_2, \delta, v)I_2, \tag{7}$$

where I_1 and I_2 are the intensities of the counterpropagating (pumping) and probe waves, respectively. In the case of atomic gas, the absorption coefficient α should be averaged over the velocity (Maxwell) distribution:

$$\langle\alpha\rangle_v = \frac{1}{\sqrt{2\pi}\,v_0}\int_{-\infty}^{\infty}\alpha(v)\exp\left(-\frac{v^2}{v_0^2}\right)\mathrm{d}v. \tag{8}$$

Here v_0 is the most probable thermal velocity of the atom in gas. Later on, the symbol $\langle\ldots\rangle_v$ will denote averaging of a certain function $f(v)$ over the Maxwell distribution, similarly to (8).

Based on the Maxwell and Lindblad equations (2), in the conditions of an optically thin medium, the change in the probe wave intensity after passing through a cell of length L can be written as

$$\Delta I = I_2 - I_{2L} \approx \langle\alpha\rangle_v I_2 L = 2\hbar\omega n L\gamma_{12} \times\langle S_2(\mathrm{Tr}[\hat{V}_2^{\dagger}\hat{V}_2\hat{\rho}^g] - \mathrm{Tr}[\hat{V}_2\hat{V}_2^{\dagger}\hat{\rho}^e])\rangle_v = \hbar\omega n L\langle\eta\rangle_v, \tag{9}$$

where

$$S_j = \frac{R_j^2}{\gamma_{12}^2 + \delta_j^2}\ (j = 1,2) \tag{10}$$

is the saturation parameter; n is the concentration of atoms; $\hat{V}^{\dagger}$ is the Hermitian conjugate matrix; $\delta_{1,2} = \delta \mp kv$ are the detunings of wave frequencies from the frequency of the

atomic transition with Doppler shifts taken into account (k and v are the projections of the atomic velocity $\boldsymbol{v}$ and the wave vector $\boldsymbol{k}$ onto the quantization axis z); and $\gamma_{12} = \Gamma + \gamma/2$ is the relaxation constant for optical coherences. Operation Tr[…] in formula (9) means the spur of a matrix. In what follows, as a signal to be analysed we will consider the value of η dependent on various parameters of the problem (v, δ, ε_1, ε_2, φ, R_1 and R_2), which is responsible for all resonance spectroscopic features of the absorption spectrum of the probe wave. For shortness, we will call η the absorption signal of the probe wave (in the case of atomic gas it will be $\langle\eta\rangle_v$).

3. Atomic transition $F_g = 1 \to F_e = 0$

In order to obtain analytical expressions for the absorption signal of a probe wave η consider a relatively simple atomic transition $F_g = 1 \to F_e = 0$, which is assumed cyclic. Later we will show that in this case the contrast double SAR structure can also be observed, whereas in the two-level atomic model the transition must necessary be open [10].

In the case of the transition $F_g = 1 \to F_e = 0$, as opposed to $F_g = 0 \to F_e = 1$, one may a priori assume that the polarisation parameters of counterpropagating waves substantially affect the spectroscopic signal, in particular, the contrast of the double SAR structure. Indeed, in the case of the degenerated ground state ($F_g \neq 0$), nonlinear resonances may be subjected to a strong influence of the optical pumping, namely, redistribution of populations between magnetic sublevels of the ground state. This influence may occur even at weak saturation fields ($S \ll 1$). In turn, it is obvious that the effects of optical pumping strongly depend on the polarisation parameters of light waves.

Generally, for the considered transition, the system of equations written in the matrix form (2) may comprise 16 unknowns, that is, the dimension of the density matrix (3) is 4×4. However, the dimensionality of the system can easily reduced, for example, by excluding optical coherences. In addition, in the case of simple configurations of field polarisations, system (2) may take a rather simple form. However, we dwell on mathematical details and start with analysis of analytical results.

Note that we do not use the theory of perturbations with respect to a small intensity of the probe wave for obtaining the analytical expressions, because we are interested, first of all, in the regimes where the intensities of the counterpropagating waves are comparable. Nevertheless, for arbitrary parameters of wave polarisations, the expressions for the absorption signal η are cumbersome and inconvenient for a qualitative analysis. Hence, we will first consider the simplest particular cases of wave polarisations (linear and circular) and in the general case of elliptical polarisations we will present results of numerical calculations.

3.1. Counterpropagating waves with similar circular polarisations

Due to the symmetry of the problem it is obvious that the results for the waves with a similar right circular polarisation ($\sigma^+\sigma^+$ configuration) will not differ from those for the waves with similar left circular polarisations ($\sigma^-\sigma^-$ configuration) for an arbitrary transition $F_g \to F_e$. For definiteness, we may consider the $\sigma^+\sigma^+$ field. A scheme of induced and spontaneous transitions is given in Fig. 3. For convenience, we introduce the following notations for the energy sublevels: $|F_g = 1, m_g = -1\rangle = |1\rangle$, $|F_g = 1, m_g = 0\rangle = |2\rangle$, $|F_g = 1, m_g = +1\rangle = |3\rangle$; and $|F_e = 0, m_e = 0\rangle = |0\rangle$.

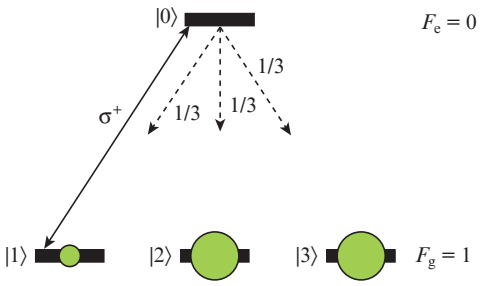

Figure 3. Atomic transition $F_g = 1 \to F_e = 0$. Here and in Figs 6, 9, 10 and 12, the solid double arrow refers to the light-induced transition; dashed arrows show possible channels of spontaneous decay with equal probability of 1/3. Circles schematically show the stationary distribution of atoms over magnetic sub-levels of the fundamental state, from which one can see that the angular atomic momenta are strongly oriented.

By solving system (2) at the parameters of ellipticity $\varepsilon_1 = \varepsilon_2 = \pi/4$, we obtain the simple expression for the absorption signal of the probe wave:

$$\eta = \frac{(2/9)\gamma_{12}S_2}{1 + 2\chi_1(S_1 + S_2)}, \tag{11}$$

where

$$\chi_1 = \frac{1}{3}\frac{\gamma_{12}[2\Gamma + (2/3)\gamma]}{\Gamma(\Gamma + \gamma)}. \tag{12}$$

Formula (11) comprises terms, which describe both the self-saturation effect (S_2 in the denominator) and the effect of cross saturation from the counterpropagating wave (the summand with S_1). Conventionally, in gas spectroscopy experiments, the condition $\gamma \gg \Gamma$ is fulfilled, and one may take $\chi_1 \gg 1$. Formula (11) is exactly similar to the expression obtained in [10] for the two-level atomic model with an open transition. Indeed, according to formula (19) from [10] we have

$$\eta \equiv W = \frac{2\gamma_{12}S_2}{1 + 2\chi(S_1 + S_2)}, \tag{13}$$

where

$$\chi = \frac{\gamma_{12}(2\Gamma + b\gamma)}{\Gamma(\Gamma + \gamma)}; \tag{14}$$

$b = 1 - \beta$ is the coefficient of openness for the atomic transition; and β is the branching factor (in particular, $b = 0$ corresponds to a cyclic transition).

The numerical factors 1/9 in (11) and 1/3 in (12) are exclusively related to the fact that for a real transition $F_g = 1 \to F_e = 0$ one should take into account Clebsch–Gordan coefficients [9, 36], which are absent in the model (13), (14) of a two-level atom [10]. Hence, the configuration $\sigma^+\sigma^+$ (and $\sigma^-\sigma^-$) of the field interacting with the cyclic transition $F_g = 1 \to F_e = 0$ completely corresponds to the two-level atomic model studied in [10]. Moreover, a comparison of formulae (12) and (14) yields that for such a transition there is a certain effective coefficient of openness $b = 2/3$. This is an obvious value because b indicates how many atoms initially excited from level $|1\rangle$ and then spontaneously relaxed from excited

level $|0\rangle$ do not return back to level $|1\rangle$. From Fig. 3 immediately follows $b = 2/3$.

Obviously, the field configurations $\sigma^+\sigma^+$ and $\sigma^-\sigma^-$ facilitate observation of a contrast double SAR structure (at $R_2 > R_1$), which is illustrated in Fig. 4. The dependences have been obtained by averaging numerically the signal η over the velocity distribution of atoms according to (8). In all the calculations, we take $\Gamma = 10^{-3}\gamma$, which by the order of magnitude corresponds to standard experimental conditions in spectroscopy of vapours of alkali metals at room temperature at the diameter of a laser beam of ~5 mm.

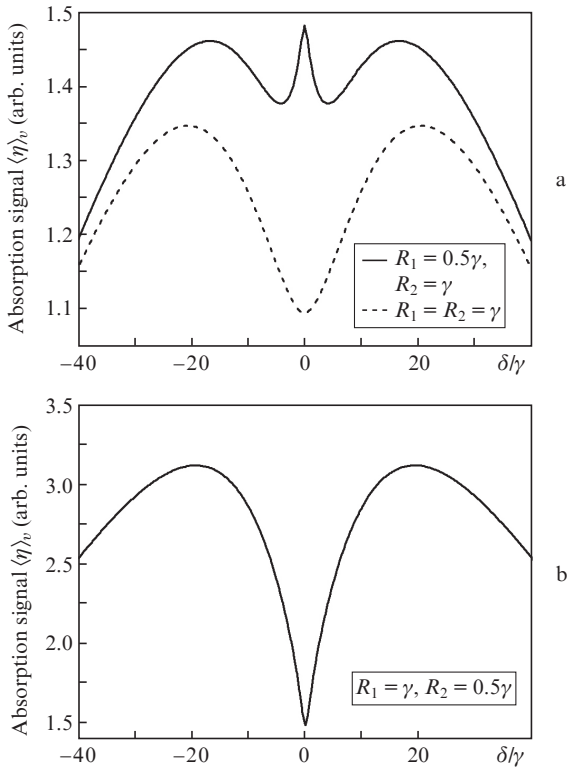

Figure 4. Signals of the probe wave absorption by all velocity groups of atoms $\langle\eta\rangle_v$ vs. the frequency detuning for the field configuration $\sigma^+\sigma^+$ in the regime of a standing wave and a double structure (a), the pump-probe regime (b).

In view of the similarity of formulae (11), (12) and (13), (14), which is a consequence of the two-level atomic model, the mathematical background of the arising double SAR structure in our case (the $\sigma^+\sigma^+$ or $\sigma^-\sigma^-$ configuration) is the same as in [10]. In particular, from this background follows that the contrast double SAR structure can be only observed at $R_2 > R_1$. However, in the present work we will focus our attention on a qualitative interpretation of SAR. Such interpretation is also given in [10]; it, naturally, remains valid for the considered field configuration. However, for studying the effect at other wave polarisations (see below) we should improve the theory in order to understand the absence of the double structure effect at certain polarisations. First, we will briefly recall the qualitative interpretation of the effect given in [10] for the considered case.

Thus, we use formulae (8) and (11) to analyse qualitatively physics of the double SAR structure formation. Consider dependences of the signal of probe wave absorption η on the atomic velocity taking into account the Maxwell distribution, that is, $\tilde{\eta}(v, \delta, R_1, R_2) = \eta(v, \delta, R_1, R_2)\exp[(-v/v_0)^2]$. Let us analyse the form of these functions for two fixed values of the detuning: $\delta = 0$ (exact resonance) and $\delta = 5\gamma$ (near the central resonance). For comparison, in Fig. 5, dependences $\tilde{\eta}(v)$ are presented in two regimes: the standing wave regime with $R_1 = R_2 = \gamma$ and the regime with $R_2 = \gamma > R_1 = 0.5\gamma$ (the probe wave is more intensive than the counterpropagating pumping wave). The solid curve corresponds to the case $\tilde{\eta}(v, \delta = \text{const} \neq 0, R_1 = \text{const}, R_2 = \text{const})$, the dashed curve is the same dependence without a pumping wave ($R_1 = 0$), and the dash-and-dot curve refers to the case of the exact resonance $\tilde{\eta}(v, \delta = 0, R_1 = \text{const}, R_2 = \text{const})$. Note that according to (8) the area under each curve corresponds to the coefficient of probe wave absorption by all velocity groups of atoms, that is, by all gas, at the prescribed frequency detuning.

From Fig. 5a one can see that at $\delta \neq 0$ there are two factors, which oppositely affect the area under the curve: increase the absorption of the probe wave for the group of atoms with $kv \approx -\delta$ and reduce the absorption for the atoms with a Doppler shift $kv \approx +\delta$. Physics of this behaviour of $\tilde{\eta}(v)$ is rather simple. Recall that in the configuration $\sigma^+\sigma^+$ at $\delta = 0$ (at the centre of the resonance) both counterpropagating waves are involved in the optical pumping of the same atoms to off-resonance sublevels of the ground state $|2\rangle$ and $|3\rangle$ (so-called pockets, see Fig. 3). At $\delta \neq 0$, both waves resonantly interact with various velocity groups of atoms in gas. Thus, atoms with $kv \approx -\delta$ mainly interact with the probe wave, because they are matched with it ($\delta_2 = 0$). In this group of atoms the probe wave is absorbed stronger than in the group

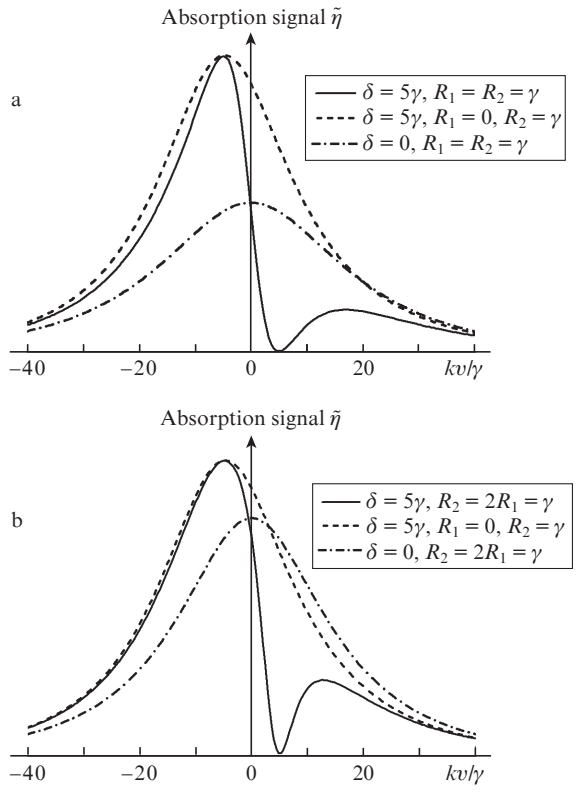

Figure 5. Signals of probe wave absorption $\tilde{\eta}$ vs. the atomic velocity (Doppler shift) for the field configuration $\sigma^+\sigma^+$ in the standing wave regime (a) and in the regime where the probe wave is more intensive than the pumping wave (b).

with $kv = 0$ (at $\delta = 0$), because in the latter case, atoms actively interact with the pumping wave as well, which results in a certain bleaching of the transition for the probe wave. A noticeable dip in the absorption spectrum of the probe wave in Fig. 5a near $kv \approx +\delta$ is related to that this velocity group of atoms interacts with the resonance pumping wave and the pumping wave is mainly absorbed in these atoms and participates in distributing atoms over the magnetic sublevels of the ground state.

Thus, the two factors have been found which affect oppositely the total area under the curve $\tilde{\eta}(v)$ in Fig. 5,a. The influence of these factors is different. Namely, the dip near $kv \approx +\delta$ (see the solid curve) reduces the total area at a less degree than the peak at $kv \approx -\delta$ increases this area, because the dip resides in a tail of the profile $\tilde{\eta}(v)$. The resulting effect of these two factors is the total increase of the area under the curve $\tilde{\eta}(v)$, which increases the absorption of the probe wave if the exact resonance ($\delta = 0$) is absent. In this way, a conventional SAR dip is formed (see Fig. 4a, dashed curve).

Obviously, at a greater detuning, the absorption of the probe wave will stop growing because the number of resonance atoms in gas falls proportionally to $\exp\{-[\delta/(kv_0)]^2\}$. Thus, a wide 'Doppler' profile of the spectroscopic signal is formed (see Fig. 4).

Consider the case of $R_2 > R_1$. Similar dependences of the absorption signal $\tilde{\eta} = \eta\exp[-(v/v_0)^2]$ are shown in Fig. 5b. One can see that in this case the factor, which reduces the absorption, only slightly increases the area under the curve, that is, the maxima of the absorption signal at $\delta = 0$ and 5γ (dash-and-dot and solid curves) do not differ so much as in the case of a standing wave (Fig. 5a). However, the dip in the absorption spectrum near $kv \approx +\delta$ is still noticeable. Such a moderate difference in the maxima of absorption signals $\tilde{\eta}(v)$ at $\delta = 0$ and 5γ is related to the fact that in both cases the probe wave interacts with resonance atoms stronger than the counterpropagating wave does. That is, in the regime $R_2 > R_1$, the counterpropagating wave weakly affects the absorption of the probe wave by resonance groups of atoms. On the contrary, in the velocity group of atoms with $kv \approx +\delta$, as earlier, the pumping wave bleaches the transition, which, in contrast to the probe wave, is in resonance with this group of atoms. Hence, by comparing the areas under the curves in the case of exact resonance ($\delta = 0$) and near it ($\delta = 5\gamma$) one can see that the absorption of the probe wave falls – in this way a peak at the centre of resonance is formed (see Fig. 4a, solid curve). With increasing detuning, similarly to the case of a standing wave, the dip in the solid curve in Fig. 5b shifts to the tail and stops to noticeably reduce the area under the curve. In this case, the factor leading to a greater absorption near $kv \approx -\delta$ becomes determining, and the absorption of the probe wave by all gas becomes greater with an increase in detuning. In this way, an ordinary SAR dip is formed. Hence, physics of origin of the double SAR structure in the regime $R_2 > R_1$ becomes clear.

3.2. Counterpropagating waves with parallel linear polarisations

This case is also sufficiently simple for analysis. However, it is more convenient to choose the quantization axis z along the vectors of the linear polarisation rather than along the wave propagation direction. Then the scheme of induced and spontaneous transitions will look like shown in Fig. 6. Instead of the orientation of angular momenta as in Fig. 3, now a strong alignment to extreme magnetic sublevels of the ground state is

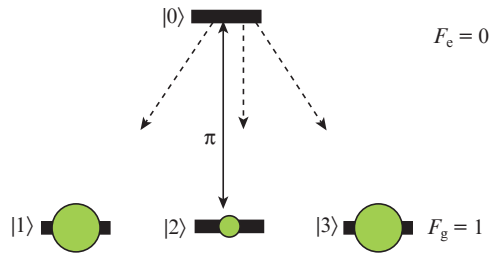

Figure 6. Transition $F_g = 1 \rightarrow F_e = 0$ in the atom interacting with a field of the counterpropagating waves with parallel linear polarisations (the quantization axis is directed along the polarisation vectors).

observed due to the induced transitions of the π-type and to the optical pumping.

From Fig. 6, one can see that this configuration is very similar to that considered in Section 3.1. Indeed, in this case the counterpropagating waves also interact with the common transition, which includes only two magnetic sublevels, i.e. $|0\rangle$ and $|2\rangle$, whereas the optical pumping excites levels $|1\rangle$ and $|3\rangle$. It is intuitively obvious that a spectroscopic signal in such a scheme will be similar to the signal with the field configuration $\sigma^+\sigma^+$ (Fig. 3). This conclusion is confirmed by direct calculations, which yield the same formula for the absorption signal as (11). Hence, in a scheme with parallel linear polarisations of counterpropagating waves (the configuration lin∥lin) observation of the double SAR structure is also possible.

3.3. Counterpropagating waves with orthogonal circular polarisations

Consider now the field with the configuration $\sigma^+\sigma^-$, which in our problem is equivalent to the field with the $\sigma^-\sigma^+$ configuration. As will be shown below, this configuration principally differs from the configurations considered earlier. By solving system (2) for the $\sigma^+\sigma^-$ configuration we obtain the expression:

$$\eta = \frac{(2/9)\gamma_{12}S_2\{1 + [2\gamma_{12}/(3\Gamma)]S_1\}}{1 + 2\chi_1(S_1 + S_2) + 4\chi_2 S_1 S_2}, \tag{15}$$

where

$$\chi_2 = \frac{\gamma_{12}^2}{27\Gamma^2}\left(1 + \frac{8\Gamma}{\gamma + \Gamma}\right). \tag{16}$$

Formula (15) qualitatively differs from expression (11), in particular, by the summand with S_1S_2; hence, in this case one may expect a substantially different spectrum of the signal as compared to the field configurations considered previously. In ordinary experimental conditions ($\gamma \gg \Gamma$) the relationship $\chi_1 \gg 1$ holds. Note that in the regime of small saturation, formula (15) agrees with expression (2) from [34] if we take I_1, $I_2 \ll 1$.

As earlier, we will study features of the function $\tilde{\eta}(v, \delta, R_1, R_2)$ at fixed R_1, R_2 and δ. The corresponding dependences are presented in Fig. 7, where one can see the absorption spectrum without any dip near $kv \approx +\delta$, unlike to the dependences in Fig. 5. Moreover, one can see that both in the regime of a standing wave and regime with $R_2 > R_1$, the profiles of the probe wave absorption at $\delta = 5\gamma$ are below the profile corresponding to $\delta = 0$. This results in the formation of a peak at the centre of the resonance. In the cases of $\sigma^+\sigma^+$,

$\sigma^-\sigma^-$, and lin$\|$lin configurations, at increasing δ, the formation of the peak stopped and a dip started to reveal in the dependence $\langle\eta\rangle_v$; that is, the double structure of nonlinear resonance was formed (see Fig. 4a, the solid curve). The reason for the dip formation was disappearance of the 'hole' in the profile $\tilde{\eta}(v)$ near $kv \approx +\delta$. However, since no such hole is formed in the configuration $\sigma^+\sigma^-$ at all (at any δ), at a greater detuning of laser field frequency the total coefficient of absorption (by all gas) for the probe wave still reduces. In this case one can assert that all nonlinear contributions near the centre of a spectroscopic signal have the same sign and overlap. All these features result in that in the cases of $\sigma^+\sigma^-$ or $\sigma^-\sigma^+$ wave polarisations the double SAR structure is absent (Fig. 8).

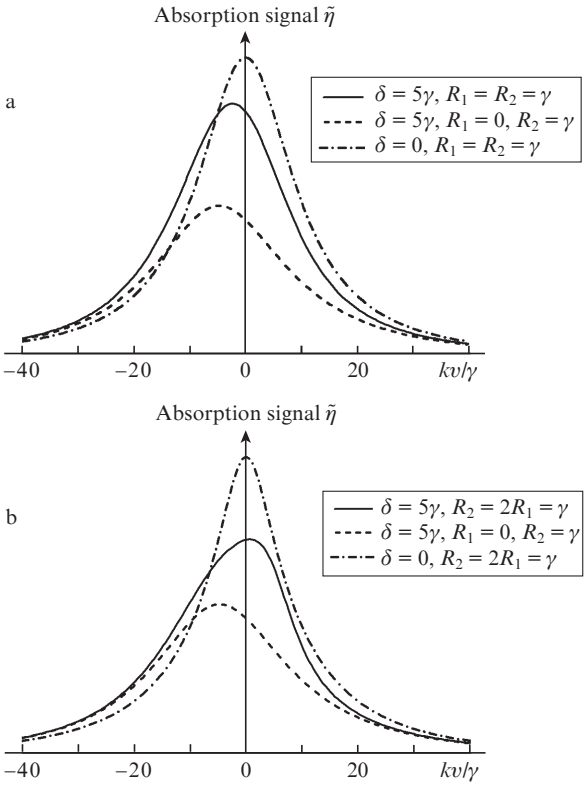

Figure 7. Signals of the probe wave absorption $\tilde{\eta}$ vs. the atomic velocity (Doppler shift) for the field configuration $\sigma^+\sigma^-$ in the standing wave regime (a) and in the regime, where the probe wave is more intensive than the pumping wave (b).

Physical reasons for the absence of a dip at all frequency detunings near $kv \approx +\delta$ in the dependences in Fig. 7 (solid curves) are also clear. A scheme of the corresponding atomic transitions is shown in Fig. 9. Indeed, the probe wave, which in this case has the polarisation σ^-, induces the transition $|3\rangle \leftrightarrow |0\rangle$. Part of atoms in such interaction still does not return back to level $|3\rangle$ due to spontaneous decays to levels $|1\rangle$ and $|2\rangle$. The counterpropagating wave with the polarisation σ^+ (pumping), both at $\delta = 0$ (dash-and-dot curves in Fig. 7) and at $\delta = 5\gamma$ (solid curves), acts on the atomic groups with $kv \approx \pm\delta$ in both interaction regimes ($R_1 = R_2$ and $R_2 > R_1$) in such a way that to return only a part of atoms from level $|1\rangle$ to level $|3\rangle$. The return leads to the additional absorption of the probe wave, and hence in both regimes (Figs 7a and 7b) the dashed curves are below solid curves as at $kv \approx -\delta$ so and at $kv \approx +\delta$.

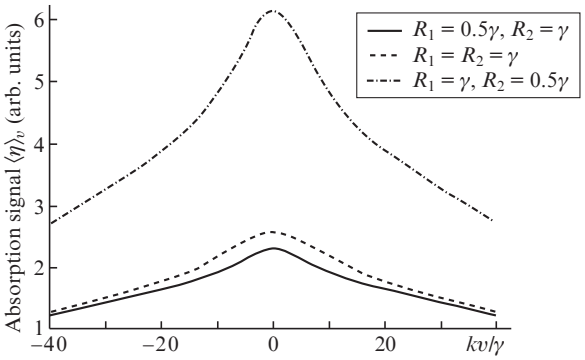

Figure 8. Signals of the probe wave absorption by all atomic velocity groups $\langle\eta\rangle_v$ vs. the frequency detuning for the field configuration $\sigma^+\sigma^-$ in three regimes with various field intensities: the pump-probe regime (dash-and-dot curve), standing-wave regime (dashed curve) and regime where the probe wave is more intensive than the pumping wave ($R_2 > R_1$) (solid curve).

Thus, the qualitative analysis of the spectroscopic signal in the case of $\sigma^+\sigma^-$ makes us to conclude that no double SAR structure is formed. Also, there is no conventional SAR dip; however, a peak at the centre of the signal is observed. Similar results are also presented in [7].

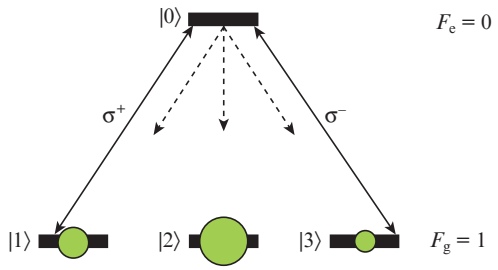

Figure 9. Transition $F_g = 1 \rightarrow F_e = 0$ in the atom interacting with a field of the counter-propagating waves possessing opposite circular polarisations (the quantization axis is directed along the wave vectors). A qualitative stationary distribution of atoms over the magnetic sub-levels corresponds to the case of $R_2 > R_1$.

3.4. Counterpropagating waves with orthogonal linear polarisations

This configuration is of particular interest, because each of the counterpropagating waves can 'pump' atoms to a specific coherent state – the 'dark' state which is a superposition of states $|1\rangle$ and $|3\rangle$. This state can be formed due to a quantum interference of the σ^+ and σ^- transitions induced by each of the waves (Fig. 10). The specificity of this dark state is that the atoms, 'pumped' by a light wave to this state, cease scattering the energy of this wave and make the medium transparent (see pioneering works [37–39]). This phenomenon is called the coherent population trapping (CPT). Here we will not discuss essentials of the CPT theory; instead, we suggest reading a review [40].

Let us emphasise one more important feature of the configuration with orthogonal linear polarisations of counterpropagating waves (the lin$\perp$lin configuration). As was mentioned, each of the waves separately can form a CPT state. However, for each of the waves this state is different.

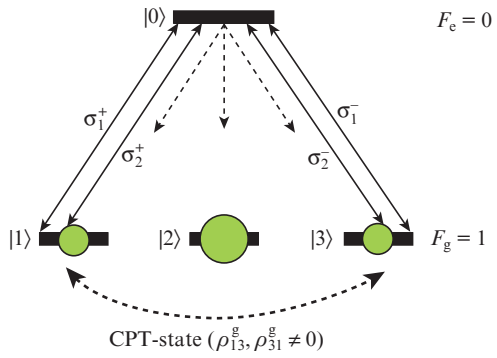

Figure 10. Transition $F_g = 1 \to F_e = 0$ in the atom interacting with a field of the counterpropagating waves possessing orthogonal linear polarisations (the quantization axis is directed along the wave vectors). Each of the waves participates in forming the superimposed states $|1\rangle$ and $|3\rangle$ in the result of σ^+ and σ^- transitions (dashed bent arrow shows formation of such superposition – Zeeman coherence).

Moreover, the dark state for the wave $\boldsymbol{E}_1$ is 'bright' for wave $\boldsymbol{E}_2$ (that is, leads to a strong absorption of the second wave). In the case where both the waves affect the same atoms in gas and have equal intensities, these CPT states are orthogonal, that is, compete with each other so that the Zeeman coherence does not arise at all. Thus, the new superimposed state with the mentioned properties, at first glance, complicates the physics of atom–field interaction, in particular, a qualitative analysis of the double SAR structure.

First, we analyse the analytical expression for the absorption signal η as it was made previously for other field configurations. By solving system (2) we arrive at the new expression:

$$\eta = \frac{(2/9)\gamma_{12} S_2 \{1 + [\gamma_{12}/(3\Gamma)][S_1 + S_2 + \xi(S_1 - S_2)]\}}{1 + 2\chi_1(S_1 + S_2) + \chi_2[(S_1 + S_2)^2 - \xi(S_1 - S_2)^2]}. \quad (17)$$

Here, we introduced an auxiliary parameter ξ, which can take only two values 0 or 1. It gives one a possibility to exclude artificially the origin of Zeeman coherence in the ground state and to 'switch off' the influence of the CPT state on a spectroscopic signal ($\xi = 0$ corresponds to the 'switched-off' CPT effect).

By taking $\xi = 0$ in (17) we obtain

$$\eta = \frac{(2/9)\gamma_{12} S_2 \{1 + [\gamma_{12}/(3\Gamma)](S_1 + S_2)\}}{1 + 2\chi_1(S_1 + S_2) + \chi_2(S_1 + S_2)^2}. \quad (18)$$

Consider the case of small frequency detunings and low atomic velocities, that is, kv and $\delta \sim \gamma$. Dependences of the absorption signal η for R_1, $R_2 \sim \gamma$ have been presented. In those conditions, the saturation parameters S_1 and S_2 are approximately 1. Taking into account formulae (11), (12), (16), (18) and the condition $\gamma \gg \Gamma$, we arrive at the following approximate expressions for the absorption signal η in the configurations lin⊥lin and $\sigma^+\sigma^+$, respectively:

$$\eta(\text{lin}\perp\text{lin}) = \frac{2\Gamma S_2}{S_1 + S_2}, \quad (19)$$

$$\eta(\sigma^+\sigma^+) = \frac{(\Gamma/2) S_2}{S_1 + S_2}. \quad (20)$$

Thus, at low velocities of atoms, the absorption signals of these two configurations behave similarly (within the accuracy of a factor 4). Hence, one may expect that at the 'switched-off' CPT effect, a hole in the profile $\tilde{\eta}(v)$ will be burnt near $kv \approx +\delta$ as in the case of the $\sigma^+\sigma^+$ configuration (see Fig. 5).

Now, let us 'switch on' the CPT by setting $\xi = 1$ in (17). In the result, we obtain the formula that completely coincides with (15) for the $\sigma^+\sigma^-$ configuration, in which case, as we know, a dip in the absorption signal near $kv \approx +\delta$ is not formed. Hence, we see that the CPT effect radically changes the situation and results in the absence of the double SAR structure in the field configuration lin⊥lin.

The aforesaid can be illustrated graphically as previously. Dependences of the signal of the probe wave absorption with the 'switched off' ($\xi = 0$) and 'switched on' ($\xi = 1$) SAR effect are shown in Fig. 11. In the first case, a deep hole is burnt in the profile $\tilde{\eta}(v)$ at the detuning from the exact resonance ($\delta = 5\gamma$), whereas in the second case no hole is observed. One can see that the dependences in Fig. 11a and 11b resemble similar dependences in Fig. 5b ($\sigma^+\sigma^+$ configuration) and Fig. 7b ($\sigma^+\sigma^-$ configuration), respectively.

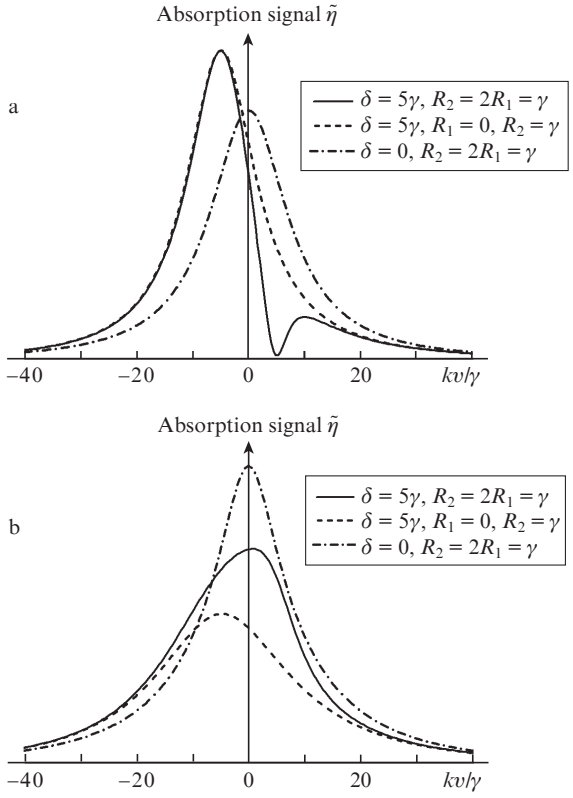

Figure 11. Signals of probe wave absorption $\tilde{\eta}$ vs. the atomic velocity (Doppler shift) for the field configuration lin⊥lin without (a) and with (b) the CPT-state formation in the regime with $R_2 > R_1$.

The analogy between the configuration lin⊥lin and configurations $\sigma^+\sigma^+$, $\sigma^+\sigma^-$ can be also explained if we analyse the scheme of induced and spontaneous transitions (Fig. 10). At $\xi = 0$, when the σ^+ and σ^- transitions do not interfere and there is no Zeeman coherence (that is, $\rho_{13}^g = \rho_{31}^g = 0$), the configuration lin⊥lin is a kind of superposition of configurations $\sigma^+\sigma^+$ and $\sigma^-\sigma^-$. In particular, consider the regime with $R_2 > R_1$ where the double SAR structure is formed in the $\sigma^+\sigma^+$ or $\sigma^-\sigma^-$ field (see Section 3.1). At $\delta = 0$, for the relatively weak

pumping wave $\boldsymbol{E}_1$ and the probe wave $\boldsymbol{E}_2$, the resonance group of atoms is the same. In this group, the wave $\boldsymbol{E}_1$ optically pumps atoms to level $|2\rangle$ in addition to the pumping by the stronger wave $\boldsymbol{E}_2$, which reduces the absorption of the probe wave $\boldsymbol{E}_2$. At the detuning $\delta = 5\gamma$, the counterpropagating waves interact resonantly with different groups of atoms: the wave $\boldsymbol{E}_2$ interacts stronger with the group $kv \approx -\delta$, whereas the pumping wave interacts with the group $kv \approx +\delta$. Similarly to the field configuration $\sigma^+\sigma^+$, the absorption of the probe wave increases in the group $kv \approx -\delta$ because the influence of the wave $\boldsymbol{E}_1$ becomes weaker. Hence, the maximum of the solid curve in Fig. 11a is above the maximum of the dash-and-dot curve. Similarly to the case of the $\sigma^+\sigma^+$ transition, a dip arises in the spectrum of the absorption of probe wave $\boldsymbol{E}_2$ by the group of atoms with $kv \approx +\delta$ because, in this group, the wave $\boldsymbol{E}_1$ strongly affects the atomic transition and 'bleaches' it. Thus, at $\xi = 0$, the physical processes, on the basis of which the curves in Fig. 11a have been obtained, are absolutely the same as in the case of the $\sigma^+\sigma^+$ field configuration.

At $\xi = 1$, Zeeman coherences ρ_{31}^{g} and ρ_{13}^{g} arise. If the influence of the pumping wave $\boldsymbol{E}_1$ is assumed weak, that is, not destroying the Zeeman coherence formed by the wave $\boldsymbol{E}_2$, then the CPT state itself also becomes a 'trapping' state for the probe wave, similarly to the magnetic sublevel $|2\rangle$. Hence, at $\delta = 5\gamma$, the absorption of the probe wave by the resonance group of atoms with $kv \approx -\delta$ is weaker than at $\delta = 0$, when the CPT states of both the waves stronger compete with each other. The reason of the absence of the dip in the spectrum of the probe wave absorption by the group of atoms with $kv \approx +\delta$ also becomes obvious, because in this velocity group the pumping wave $\boldsymbol{E}_1$ produces the superimposed state, which is bright for the wave $\boldsymbol{E}_2$. This results in an increase of the absorption rather than in a reduction.

It is convenient to analyse the influence of the CPT state on the possibility of observing the double SAR structure not in the basis of eigen-states of the Hamiltonian of the free atom $\hat{H}_0$, with which we dealt so far, but in the new orthonormal basis

$$\left\{|C\rangle = \frac{1}{\sqrt{2}}(|1\rangle + |3\rangle), |\mathrm{NC}\rangle = \frac{1}{\sqrt{2}}(|1\rangle - |3\rangle), |2\rangle, |0\rangle\right\}. \qquad (21)$$

In this basis, the dimensionless operators of the interaction of counterpropagating waves with the atomic transition $F_g = 1 \rightarrow F_e = 0$ take the simple form (in the configuration lin⊥lin):

$$\hat{V}_1 = -\frac{1}{\sqrt{3}}|0\rangle\langle \mathrm{NC}|, \qquad (22)$$

$$\hat{V}_2 = \frac{\mathrm{i}}{\sqrt{3}}|0\rangle\langle \mathrm{C}|. \qquad (23)$$

From formulae (21)–(23) immediately follows that the superimposed state $|\mathrm{NC}\rangle$ (uncoupled) is dark for the probe field $\boldsymbol{E}_2$, that is,. $\hat{V}_2|\mathrm{NC}\rangle = 0$. On the contrary, the state $|\mathrm{C}\rangle$ is dark for the pumping wave, but bright for the probe wave, that is, $\hat{V}_1|\mathrm{C}\rangle = 0$ and $\hat{V}_2|\mathrm{C}\rangle \neq 0$. A scheme of atomic transitions in the new basis is given in Fig. 12. One can see that the field $\boldsymbol{E}_1$ interacts with only two levels $|\mathrm{NC}\rangle$ and $|0\rangle$, and the field $\boldsymbol{E}_2$ interacts with levels $|\mathrm{C}\rangle$ and $|0\rangle$. Each of the waves optically pumps two sublevels of the ground state as well. Note that the scheme in Fig. 12 is similar to that in Fig. 9. Hence, the spectroscopic signals for the configurations lin⊥lin and $\sigma^+\sigma^-$ are identical.

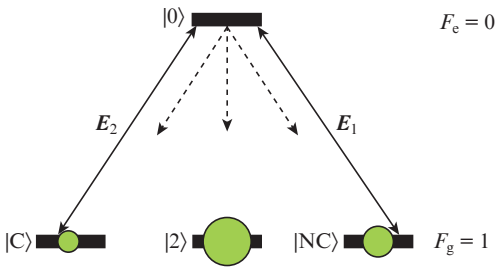

Figure 12. Transition $F_g = 1 \rightarrow F_e = 0$ in the atom interacting with a field of the counterpropagating waves possessing orthogonal linear polarisations (stationery states of atom are presented in the new basis). A qualitative stationary distribution of atoms over the magnetic sub-levels corresponds to the case of $\delta = 0$, $R_2 > R_1$.

3.5. Arbitrary elliptical polarisations

So far we have considered particular and relatively simple polarisation configurations of the field. These configurations are more often used in practice. However, for completeness of knowledge about the influence of polarisation parameters of fields on the formation of the double SAR structure we will briefly present calculation results concerning arbitrary elliptical polarisations.

In Fig. 13a, dependences are shown of the signal of probe wave absorption by atomic gas versus the frequency detuning for the waves with similar elliptical polarisations ($\varepsilon_1 = \varepsilon_2 = \pi/10$) and for the waves with the elliptical parameters equal in absolute values but rotating oppositely ($\varepsilon_1 = -\varepsilon_2 = \pi/10$). The principal axes of the ellipses are assumed parallel, that is,

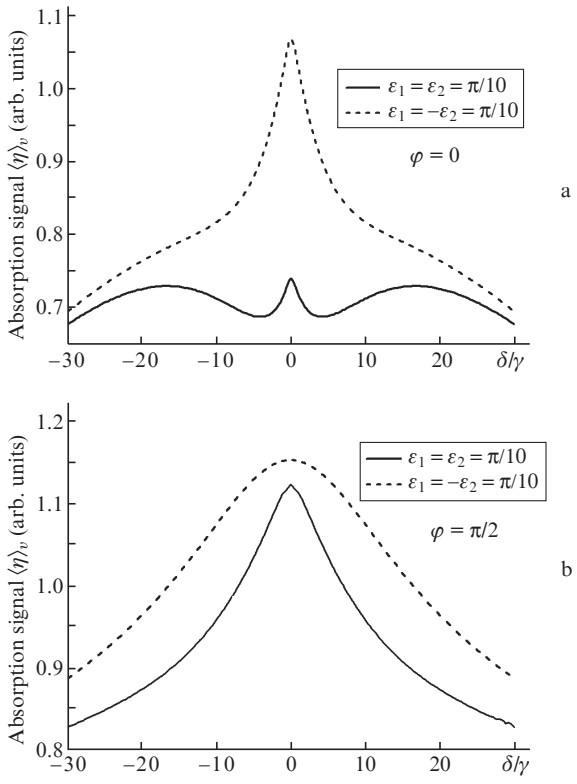

Figure 13. Signals of probe wave absorption by atomic gas $\langle\eta\rangle_v$ vs. the frequency detuning for different configurations of the fields of counterpropagating elliptically polarised waves for parallel (a) and orthogonal (b) principal axes of polarisation ellipses in the regime with $R_1 = 0.5R_2 = \gamma$.

$\varphi = 0$. From the figure it follows that the sense of rotation of the polarisation vector for elliptically polarised waves is also important, as it was in the case of $\sigma^+\sigma^+$- and $\sigma^+\sigma^-$ configurations: in the first case, a contrast double structure is observed, and in the second case such a structure is absent. In Fig. 13b one can see the same dependences as in Fig. 13a for the case of orthogonal elliptical polarisations ($\varepsilon_1 = \varepsilon_2 = \pi/10$, $\varphi = \pi/2$, and $\varepsilon_1 = -\varepsilon_2 = \pi/10$, $\varphi = \pi/2$).

As follows from the dependences shown in Fig. 13, the central peak in the case of the double SAR structure is narrower as compared to the resonance curves observed without the double structure. Thus, the regime of the double SAR structure may be of particular importance in nonlinear laser spectroscopy and its applications, for example, in stabilising a laser radiation frequency. In addition, a new problem arises: determination of the polarisation parameters of counterpropagating waves (ε_1, ε_2, φ), at which the double SAR structure arises and the central peak has a maximal contrast, for example, with respect to the dip. Naturally, for different atomic dipole transitions ($F_g \to F_e$) it is necessary to find a particular set of such polarisation parameters. This set will also depend on the wave intensities (R_1, R_2). Here we briefly present calculation results for the transition $F_g = 1 \to F_e = 0$ at $R_1 = 0.5R_2 = \gamma$.

In Fig. 14 we present calculation results for the ratio of the central peak amplitude to the amplitude of the dip in a spectrum of saturated absorption (see Fig. 13a, the solid curve) at ε_1, $\varepsilon_2 \geqslant 0$and $\varphi = 0$. The picture is presented in grey halftones, where the black colour corresponds to the maximal amplitude ratio. A 'corridor' of parameters $\varepsilon_1, \varepsilon_2$, in which the double SAR structure can be observed, is clearly seen in the picture. In particular, near the line $\varepsilon_1 = \varepsilon_2$, the amplitude of the central peak is approximately equal to the amplitude of the dip (see Fig. 13a, solid curve), and farther from this line the amplitude of the dip sharply falls so that only the central peak remains, which merges with a wide 'Doppler' profile and the double SAR structure vanishes (see Fig. 13a, the dash-and-dot curve). It is important that the results of calculations of nonlinear signal parameters (the amplitude and width of the central peak, its contrast and so on) are symmetric relative to the line $\varepsilon_1 = \varepsilon_2$.

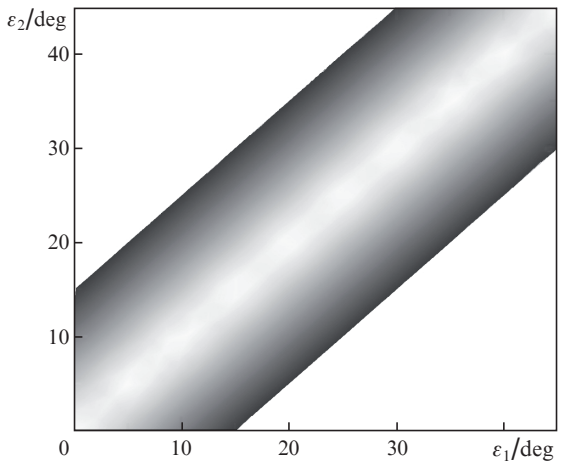

Figure 14. 'Corridor' of the parameters of ellipticity of counterpropagating waves ε_1, ε_2, within which the double SAR structure can be observed, at $R_1 = 0.5\gamma$, $R_2 = \gamma$, $\varphi = 0$.

4. Conclusions

In the present work we have investigated the effect of the double SAR structure that was first considered in [10]. The main attention was paid to the polarisation aspect of atomic gas interaction with the field of counterpropagating light waves. In [10], a qualitative understanding of physics of the new nonlinear phenomenon was based on the simplified two-level atomic model, which ignored the vector nature of light and degeneration of atomic levels with respect to the projection of the total angular momentum. We have extended the theory of the new effect as applied to the case of real atomic systems with degenerated energy levels.

The influence of the polarisation parameters of the light field on a possibility to obtain the double SAR structure was studied by an example of a simple atomic transition $F_g = 1 \to F_e = 0$ with the degenerated ground state. A strong influence of the polarisation parameters both on the contrast of the double SAR structure and on the possibility of obtaining the effect has been demonstrated. Based on the detailed analysis of analytical expressions and dependences of the absorption signal for the probe beam and on the results of numerical calculations, we have established a number of important spectroscopic laws for various configurations of light field polarisations.

The results obtained substantially supplement those of Ref. [10] and reveal new physical conditions necessary for obtaining the effect of the double SAR structure. The theoretical analysis performed, in addition to purely academic importance, is also interesting for practice, because the new nonlinear resonance can be used, for example, in transportable frequency standards based on SAR in atoms and molecules.

Note that in the present work we used the approximation of lowest spatial harmonics of atomic polarisation, which is valid at weak saturation of the atomic transition. However, actually, in using SAR this regime of weak saturation may fail, because in the conditions of optical pumping the saturation intensity is not high. Hence, further development of the theory of the double SAR structure presented above, from our point of view, should include investigation of the combined influence of polarisation parameters of light waves and higher spatial harmonics of atomic polarisation. However, the considered approximation of the lowest spatial harmonics is necessary for understanding the influence of the polarisation effects on the origin of the double SAR structure.

Acknowledgements. The work was partially supported by the Russian Foundation for Basic Researches (Grant Nos 15-02-08377, 15-32-20330 and 14-02-00939), the Ministry of Education and Science of the Russian Federation (State Research Task No. 2014/139, Project No. 825), and grants of the President of the Russian Federation (MK-4680.201402 and NSh-4096.2014.2), and the Presidium of the Siberian Branch of the Russian Academy of Sciences.

References

1. Letokhov V.S., Chebotaev V.P. *Nelineinaya lazernaya spektroskopiya sverkhvysokogo razresheniya* (Nonlinear Laser Spectroscopy of Ultra-High Resolution) (Moscow: Nauka, 1990).
2. Rautian S.G., Smirnov G.I., Shalagin A.M. *Nelineinye rezonansy v spektrakh atomov i molekul* (Nonlinear Resonances in Atomic and Molecular Spectra) (Novosibirsk: Nauka, 1970).
3. Demtroder W. *Laser Spectroscopy* (New York: Springer, 2003).

4. Lamb W.E. Jr. *Phys. Rev*., **134**, A1429 (1964).
5. Haroche S., Hartmann F. *Phys. Rev. A*, **6**, 1280 (1972).
6. Shirley J.H. *Phys. Rev. A*, **8**, 347 (1973).
7. Pappas P.G., Burns M.M., Hinshelwood D.D., Feld M.S. *Phys. Rev. A*, **21**, 1955 (1980).
8. Yudin V.I. *Dokt. Diss*. (Novosibirsk State University, 2000).
9. Brazhnikov D.V., Taichenachev A.V., Tumaikin A.M., Yudin V.I., Velichanskii V.L., Zibrov S.A. *Zh. Exp. Teor. Fiz*., **136**, 18 (2009).
10. Vasil'ev V.V., Velichanskii V.L., Zibrov S.A., et al. *Zh. Exp. Teor. Fiz*., **139**, 883 (2011).
11. Hall J.L., Borde C.J., Uehara K. *Phys. Rev. Lett*., **37**, 1339 (1976).
12. Ishikawa J., Riehle F., Helmcke J., Borde Ch.J. *Phys. Rev. A*, **49**, 4794 (1994).
13. Badalyan A.M., Kovalevskii V.I., Saprykin E.G., Sedel'nikov A.P., Smirnov G.I. *Avtometriya*, **1**, 106 (1984).
14. Lee H.S., Park S.E., Park J.D., Cho H. *J. Opt. Soc. Am. B*, **11**, 558 (1994).
15. Di Lorenzo-Filho O., Rios Leite J.R. *Phys. Rev. A*, **58**, 1139 (1998).
16. Rautian S.G., Saprykin E.G., Chernenko A.A. *Opt Spektrosk*, **104**, 630 (2008).
17. Eickhoff M.L., Hall J.L. *IEEE Trans. Instrum. Meas.*, **44** (2), 155 (1995).
18. Bagayev S.N., Dmitriyev A.K., Pokasov P.V. *Laser Phys*., **7**, 989 (1997).
19. Guo R., Hong F.-L., Onae A., Bi Z.-Y., Matsumoto H., Nakagawa K. *Opt. Lett*., **29** (15), 1733 (2004).
20. Skvortsov M.N., Okhapkin M.V., Nevskii A.Yu., Bagaev S.N. *Kvantovaya Electron*., **34**, 1011 (2004) [*Quantum Electron*., **34**, 1011 (2004)].
21. Nakayama K., Hyodo M., Ohmukai R., Watanabe M. *Opt. Commun*., **259**, 242 (2006).
22. Bykovskii Yu.A., Velichanskii V.L., Egorov V.E., Zibrov A.S., Maslov V.A. *Pis'ma Zh. Eksp. Teor. Fiz*., **19**, 665 (1974).
23. Bertinetto F., Cordiale P., Galzerano G., Bava E. *IEEE Trans. Instrum. Meas*., **50** (2), 490 (2001).
24. Heinecke D.C., Bartels A., Fortier T.M., Braje D.A., Hollberg L., Diddams S.A. *Phys. Rev. A*, **80**, 053806 (2009).
25. Kol'chenko A.P., Rautian S.G., Sokolovskii R.I. *Zh. Eksp. Teor. Fiz*., **55**, 1864 (1968).
26. Bagayev S.N., Dmitriyev A.K., Okhapkin M.V., Shalnev E.V., Skvortsov B.N., Nikulin V.A. *Laser Phys*., **6**, 226 (1996).
27. Akul'shin A.M., Velichanskii V.L., Gamidov R.G., Kazantsev A.P., Sautenkov V.A., Surdutovich G.I., Yakovlev V.P. *Pis'ma Zh. Eksp. Teor. Fiz*., **50**, 167 (1989).
28. Bagayev S.N., Chebotaev V.P. *Pis'ma Zh. Eksp. Teor. Fiz*., **16**, 614 (1972).
29. Tieri D.A., Cooper J., Christensen B.T.R., Thomsen J.W., Holland M.J. *Phys. Rev. A*, **92**, 013817 (2015).
30. Bagayev S.N., Baklanov E.V., Chebotaev V.P. *Pis'ma Zh. Eksp. Teor. Fiz*., **16**, 344 (1972).
31. Brazhnikov D.V., Taichenachev A.V., Tumaikin A.M., Yudin V.I., Zibrov S.A., Dudin Ya.O., Vasil'ev V.V. *Pis'ma Zh. Eksp. Teor. Fiz*., **83**, 71 (2006).
32. Brazhnikov D.V., Taichenachev A.V., Tumaikin A.M., Yudin V.I., Ryabtsev I.I., Entin V.M. *Pis'ma Zh. Eksp. Teor. Fiz*., **91**, 694 (2010).
33. Labeznyi D.B., Brazhnikov D.V., Taichenachev A.V., Yudin V.I. *Pis'ma Zh. Eksp. Teor. Fiz*., **148**, 1068 (2015).
34. Agrawal G.P. *Phys. Rev. A*, **29**, 994 (1984).
35. Lindblad G. *Commun. Math. Phys*., **48**, 119 (1976).
36. Varshalovich D.A., Moskalev A.N., Khersonskii V.K. *Kvantovaya teoriya uglovogo momenta* (Quantum Theory of Angular Momentum) (Leningrad: Nauka, 1975) p. 439.
37. Alzetta G., Gozzini A., Moi L., Orriols G. *Nuovo Cimento B*, **36** (1), 5 (1976).
38. Arimondo E., Orriols G. *Lett. Nuovo Cimento*, **17** (10), 333 (1976).
39. Gray H.R., Whitley R.M., Stroud C.R. Jr. *Opt. Lett*., **3** (6), 218 (1978).
40. Agap'ev B.D., Gornyi M.B., Matisov B.G., Rozhdestvenskii Yu.V. *Usp. Fiz. Nauk*, **163**, 1 (1993).